RSC Advances

ROYAL SOCIETY OF CHEMISTRY

www.rsc.org/advances

RSC Advances

Paper

Aptasensor for Simple Detection of Ochratoxin A Based on Side-by-Side Assembly of Gold Nanorods†

Received 00th January 20xx,
Accepted 00th January 20xx

DOI: 10.1039/x0xx00000x

www.rsc.org/

Xia Xu,[ab] Chengnan Xu[a] and Yibin Ying★[a]

This work describes a new optical aptasensor based on gold nanorod (GNR) side-by-side assembly for one-step determination of ochratoxin A (OTA), which is a mycotoxin identified as a contaminant in grains and wine throughout the world. DNA aptamer against OTA exhibiting high affinity and binding specificity has already been used as biorecognition elements to improve the detection performances. Here thiol-modified DNA were decorated on the side sites of GNRs acting as probes. Linker DNA containing aptamer sequences against OTA could hybridize with decorated DNA on the GNRs. It was illustrated that GNRs side by side oriented assembled through DNA hybridization in the absense of OTA, exhibiting strongly enhanced optical property. However in the presense of OTA, GNRs dispersed by specific aptamer-OTA recognition and conformational changes of aptamer. The resulted changes in the absorption spectra of GNRs easily obtained was employed for sensing. A linear correlation was demonstrated between the absorbance of GNRs at 708 nm and the concentration of OTA over the range from 0.5 to 20 ng/mL. The limit of detection obtained was 0.22 ng/mL (3σ) which could meet the demand for detection of the allowed OTA in foods according to European Commission Regulations (2 ng/g). Moreover selectivity and feasibility of the developed OTA aptasensor for red wine samples was also evaluated. And it was simple, efficient and cost-effective with only one-step detection, which would be a promising tool for toxin screening to guarantee food safety and to minimize the potential risks to human health.

Introduction

Ochratoxin A (OTA) is a mycotoxin identified as a contaminant throughout the world, existing in a wide variety of agro-produces, such as cereals, dried fruits, nuts, coffee beans, beer, wines, etc. Among the identified ochratoxins, OTA is the most prevalent and has the highest toxicity. It has been considered to be a potential carcinogen (group 2B) by the International Agency for Research on Cancer (IARC).[1] The presence of OTA in agro-products and foods may result in serious toxic effect even at very low concentration.[2] Therefore, it is highly necessary to develop reliable approach for determination of OTA, to guarantee food safety and minimize the potential risk of OTA to human and environmental health. Common analysis techniques, such as thin-layer chromatography (TLC), high-performance liquid chromatography (HPLC) and enzyme-linked immunosorbent assay (ELISA), has been well established and widely used during the past few years.[3] However more simple and cost-effective methods are still requested.

Antibodies are widely used as affinity-based recognition elements for OTA screening, but they are much expensive and unstable.[4] Aptamer has been adopted as an alternative approach to overcome the limitation of antibodies, impressed with its advantages of low cost, high chemical stability, specificity and recognition affinity.[5] Therein DNA-based aptamer has been demonstrated as a promising tool for OTA purification and determination, and high binding affinity was demonstrated.[6, 7] Different types of aptamer-based biosensors (simplified as aptasensors) have been constructed for OTA detection.[8-13] Among these, colorimetric aptasensor based on salt-induced aggregation of gold nanoparticles is one kind of the simplest strategies for rapid OTA determination.[14] OTA was directly detected using only one-step procedure. However the reported detection limit (20 nM) in this research was limited and still need further enhancement.

More recently, gold nanorods (GNRs) have received much attention due to their geometric anisotropy and unique optical properties.[15, 16] In particular, GNRs exhibit tunable longitudinal surface plasmon resonance (SPR) depending on the GNR aspect ratio.[17] Based on the above mentioned, biosensors using aggregation or competitive dispersion of GNRs were developed in previous researches.[18, 19] However unordered aggregates of anisotropic GNRs has limitation in repeatability when designed for practical sensing applications. Fortunately, GNRs can be assembled to superstructures in solution with controllable and reproducible end-to-end or side-by-side oriented configuration.[15] These assemblies present strongly

[a] College of Biosystems Engineering and Food Science, Zhejiang University, Hangzhou, 310058, PR China. E-mai: yingyb@zju.edu.cn; Tel: +86-571-88982885; Fax:+86-571-88982885.
[b] Department of Chemical Engineering, University of Michigan, Ann Arbor, Michigan 48109, USA
† Electronic Supplementary Information (ESI) available. See DOI: 10.1039/x0xx00000x

enhanced SPR responses in visible and near-infrared wavelength region compared with individual nanorod and unordered aggregation, induced by the simultaneous contributions from collective inter-particle coupling.[17] The SPR spectra will change in peak wavelength and intensity depending on number and shape of assemblies with fixed orientation and distances.[20, 21] Therefore, the controllable GNR assemblies achieved through specific interactions including biotin-strepavidin binding,[22, 23] DNA hybridization,[24-26] cysteine -lead,[27] oligonucleotides-mercury,[28, 29] and antibody-antigen recognition,[21, 30] offer great potential in nanoscopic optical sensing for research and practical purpose.

Several literatures mentioned biosensor study based on end-to-end or side-by-side GNR assemblies involving aptamer specific recognition events.[31, 32] DNA aptamer against thrombin and adenosine was reported, respectively. However aptamer immobilized on the nanorod surface may lead to insufficient binding affinity in the first case, while used for thrombin detection. Additionally small proportion of end-to-end assemblies formed if added with low concentration of thrombin, limiting its further sensing application. In the other case, side-by-side assemblies owing to electrostatic interaction would be easily disturbed by matrix interference, and may be limited in application of in real complex sample. Although aptamer-target recognition induced GNR assemblies is potential promising for aptasensor, it remains challenging to design appropriate sensor construction in order for excellent sensing performance.

In this work, taking advantages of specific OTA aptamer and controllable GNR assemblies, we developed a new optical aptasensor based on side-by-side GNR assembly for one-step simple determination of OTA. Free aptamer was designed as linker DNA dispersed in aqueous solution. GNRs decorated with complementary DNA on the side sites acted as probes. Simple procedure of one-step detection was achieved for OTA rapid screening. To our knowledge, this work presented the first aptasensor for detection of OTA based on GNR oriented assemblies. Therein the absorption intensity of GNRs at fixed wavelength was employed as sensing indicator, which could be easily obtained in laboratory without sophisticated and expensive equipment. And the analytical performance of the established approach like sensitivity and feasibility was evaluated. Compare with other measurements, it is simple, easy to operate and cost-effective. It would be promising for practical use of mycotoxin screening in agri-products and food.

Experimental

Reagents and materials

Hydrogen tetrachloroaurate (III) hydrate ($HAuCl_4 \cdot 3H_2O$), sodium borohydride ($NaBH_4$), silver nitrate ($AgNO_3$), hexadecyltrimethylammonium bromide (CTAB), L-ascorbic acid, dithiothreitol (DTT), thiol-functionalized polyethylene glycol (PEG-thiol), tris(2-carboxyethyl)phosphine (TCEP), OTA, ochratoxin B (OTB) and aflatoxin B_1/M_1(AFB_1/AFM_1) were obtained from Sigma-Aldrich. T-2 toxin, deoxynivalenol (DON) and zearalenone (ZON) were purchased from Fermentek (Jerusalem, Israel). All other chemical reagents used were of analytical grade. Ultrapure water with a resistivity of 18.2 MΩ·cm was used in the experiment (Millipore, Billerica, USA).

Table 1 DNA sequences and modifications used in aptasensor fabrication

DNA	Sequence
Linker DNA	5'-GTCTCACTGTGACTCTCGATCGGGTGTGGGTGGCGTAAAGGGAGCATCGGACA-3'
Random DNA	5'- CTAGCCCACACCCACCGCATTTCC -3'
3'-thiolated DNA	5'-AGTCACAGTGAGACTTTTTTT-C(6)-SH-3'
5'-thiolated DNA	5'-SH-C(6)-TTTTTTTCACCCGATCGAG-3'

All DNA used in this work were obtained from Sangon Biotech (Shanghai, China) Co. Ltd. And the detailed DNA sequences and modifications are listed in Table 1. The sequence of OTA aptamer (underlined) was designed according to previous literatures reported by J.A. Cruz-Aguado and G. Penner.[6, 7] A random DNA sequence (without OTA aptamer) was designed as negative control oligonucleotide.

Instruments and measurements

Transmission electron microscope (TEM) images of GNRs were both collected on a JEM-1230 transmission electron microscopy (JEOL, Tokyo, Japan). A 10 μL of GNR droplet was evaporated on a 300-mesh copper grid with carbon film at room temperature. At least 200 particles in TEM photos were calculated for the size characterization of nanorods. UV-vis (ultraviolet-visible) absorption spectra was measured using a SpectraMax M5 microplate reader with Softmax® Pro Software (Molecular Devices, Sunnyvale, USA). The scanning wavelength of absorption spectra was set from 400 to 1000 nm. GNRs was diluted to a volume of 100 μL and then added to each well to obtain its absorption spectra. Dynamic light scattering (DLS) tests were performed using a Zetasizer Nano ZS90 (Malvern Instruments, Malvern, UK) with a 633 nm laser source and a detector angle (25°C). The sample was diluted using ultrapure water before DLS measurements and tested with an average of three times.

GNR synthesis

Chemical synthesis of GNRs was achieved using seed-mediated growth method according to previous reports.[33-35] Preparation of gold seeds: 5 mL of 0.5 mM $HAuCl_4$ and 5 mL of 0.2 M CTAB was quickly mixed with 0.6 mL of freshly prepared 10 mM $NaBH_4$, strongly stirred for 3 min and then aged at 25 °C. The growth of GNRs: 70 μL of 0.079 M ascorbic acid was mixed well with 5 mL of 1 mM $HAuCl_4$, 5 mL of 0.2 M CTAB, and 0.15 mL of 4 mM $AgNO_3$, then added with 12 μL of gold seeds and left at 30 °C for 2 h. The synthesized GNRs were purified by centrifuge (10,000 rpm, 15 min) at room temperature and dissolved in 2 mL of 5 mM CTAB. The

concentration of synthesized GNRs was calculated according to our previous work.[18]

Fabrication of GNR-DNA probes

Decoration of thiolated DNA on the side surface of GNRs to fabricate GNR probes was performed based on reported procedures.[24] It was achieved upon one fact, that is the CTAB attached on the end sites of GNRs were much easier to be replaced than those on the side sites.[36] A 0.5 mL aliquot of concentrated GNRs were modified with DTT on the end sites for 8 h with a molar ratio of 10:1, and stabilized using PEG-thiol with a molar ratio of 100:1 for 3 h. After centrifugation and purification, TCEP-treated 3' and 5'-thiolated DNA (process within ESI) was added respectively, and then reacted at least 24 h at a molar ratio of 1000:1 under room temperature. The GNR-3'-DNA and GNR-5'-DNA probes were centrifuged (5,000 rpm, 10 min) and stored in 5 mM CTAB.

Optimization of linker DNA concentration

In order to obtain GNR side-by-side assemblies and study the optimal concentration of linker DNA, 25 μL of GNR-5'-DNA probes and 25 μL of GNR-3'-DNA-probes were mixed with 4 μL of linker DNA (pretreatment please see ESI) with different concentrations (resulting in final concentration of 0, 2, 5, 10, 20, 50, 100, 200, 300 and 400 nM) in ultrapure water by continuous oscillation. Then the mixture was added with 50 μL of 1 mM Tris-HCl buffer (pH 8.5), containing 10 mM $MgCl_2$, 100 mM NaCl and 0.02% sodium dodecylsulfate (SDS).[37] After that, the well-mixed reaction solution was incubated at 45 °C for 1 h, and then used for TEM, UV-vis absorption spectra and DLS measurements. As a control, random DNA with different concentrations was also used in this test replacing of linker DNA.

OTA detection

To detect OTA in Tris-HCl buffer, 25 μL of GNR-5'-DNA probes and GNR-3'-DNA-probes were mixed with 50 μL of OTA standard solution of different concentrations (0, 0.5, 1, 2, 5, 10 and 20 ng/mL), and then added with 4 μL of linker DNA in ultrapure water, resulting in a final concentration of 100 nM. The reaction solution was stirred and incubated at 45 °C for 1 h, and then used for measurements.

To evaluate the selectivity of established aptasensor, GNR-5'-DNA, GNR-3'-DNA probes and linker DNA were mixed and reacted in the presence of other common toxic mycotoxins existed in agri-products and food, including OTB, AFB_1, AFM_1, T-2 toxin, DON and ZON. The concentration of mycotoxin utilized was 10 ng/mL in Tris-HCl buffer (pH 8.5).

Pretreatment of wine samples

The red wine samples used in our experiment were purchased from local supermarket. The preparation of wine sample was established according to previous reported procedures.[38, 39] The red wine was initially spiked with the OTA stock solution to obtain a final concentration of 100 ng/mL. After that, several dilutions (concentrations of 2, 5, 10 and 20 ng/mL) were prepared with non-spiked red wine, followed by a 2h equilibration before extraction. Then the spiked red wine samples were extracted with a two-step procedure using toluene and chloroform, and mixed with the same volume of Tris-HCl buffer (pH 8.5). After complete phase separation, a given amount from top phase was taken out and used for detection as described before.

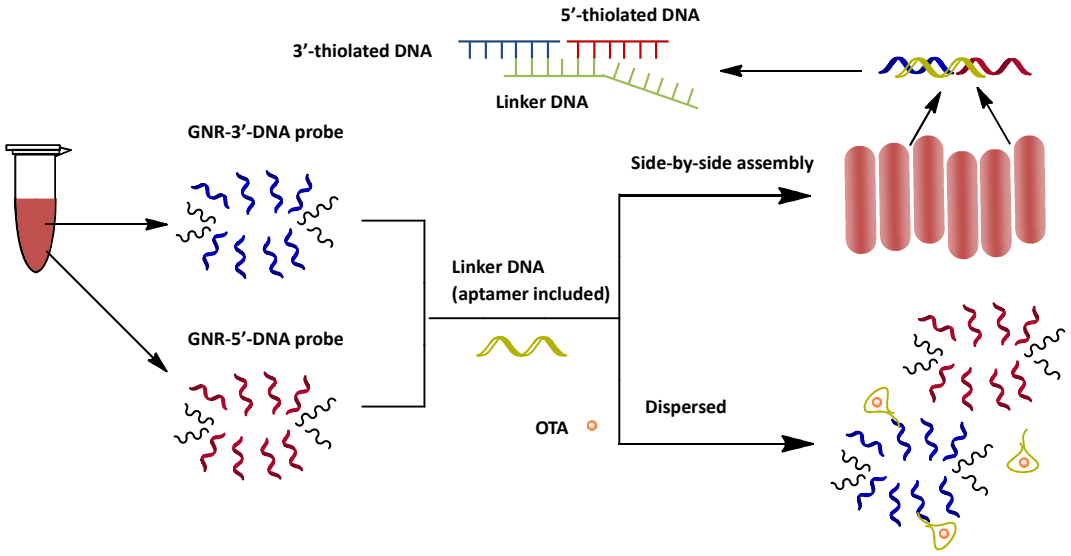

Fig. 1 Schematic illustration of OTA detection using aptasensor based on GNR side-by-side assembly

Results and discussion

Illustration of OTA aptasensor

The schematic illustration of OTA detection in this work is shown in Fig. 1 (see last section for details about preparation of GNR probes). In the absence of OTA, GNR assemblies will be observed after reaction, because two type of DNA decorated on the side sites of GNRs could hybridize with complementary linker DNA; However in the presence of OTA target, GNRs on the opposite will disperse or disassemble in solution. Because the conformational change of OTA aptamer at 3' end of linker DNA in order for specific recognition of OTA target, will result in difficulty of DNA hybridization, consequently leading to difficulty in GNR assembly.

For more details on the sensor design, the OTA-sensitive GNR assemblies consist of three components: two DNA-decorated GNR probes and a linker DNA. It was inspired by the work on aptamer-linked nanoparticle aggregates and core-shell nanorod dimmers.[40,41] The 3'-thiolated and 5'-thiolated DNA is attached to the side sites of GNRs at its 3' and 5' end, respectively. Thymine at 3' or 5' end of thiolated-DNA is designed to reduce effect of steric hindrance and improve the flexibility for oligonucleotide hybridization.[42] The linker DNA can be divided into three segments. The first and second segment hybridized with 3'-thiolated DNA and three nucleotides of 5'-thiolated DNA, respectively. The third segment as OTA aptamer, hybridized with the other nine nucleotides of 5'-thiolated DNA. In the presence of OTA molecule, the third segment of Linker DNA changes in conformational for specific recognition. Thus the three-DNA base pairs are not stable and also not strong enough to hold GNR-5'-DNA probe, leading to dispersed GNRs.

Characterization of GNR-DNA probes

The geometrical and optical properties of GNR probes were characterized TEM, UV-vis absorption spectra and DLS technique. The synthesized GNRs well dispersed in solution, had an aspect ratio of 3.1 (average length of 62 nm and average diameter of 20 nm), according to TEM image of GNRs as shown in Fig. 2. The calculated concentration of GNRs was 1.25 nM, which was significant for sensor design and following optimization of GNR assembly.

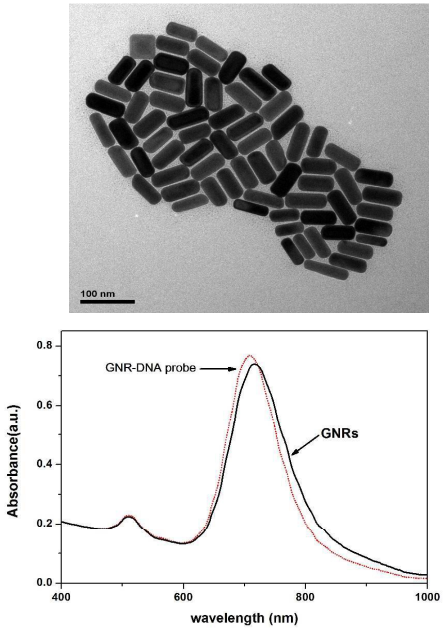

Fig. 2 TEM micrograph of synthesized GNRs and UV-vis absorption spectra of GNRs before and after DNA decoration

The UV-vis absorption spectra of GNRs and GNR-DNA probes in 5 mM CTAB was shown in Fig. 2. A blue-shift of 4 nm in longitudinal peak (from 712 nm to 708 nm) and a small red-shift of 1 nm (from 510 nm to 511 nm) in transverse peak was observed after DNA decoration. It indicated a decrease in aspect ratio of nanorods after DNA modification,[43] indicating successful decoration of thiolated DNA on the side sites of GNRs. The spectral intensity and peak shape of GNR-DNA

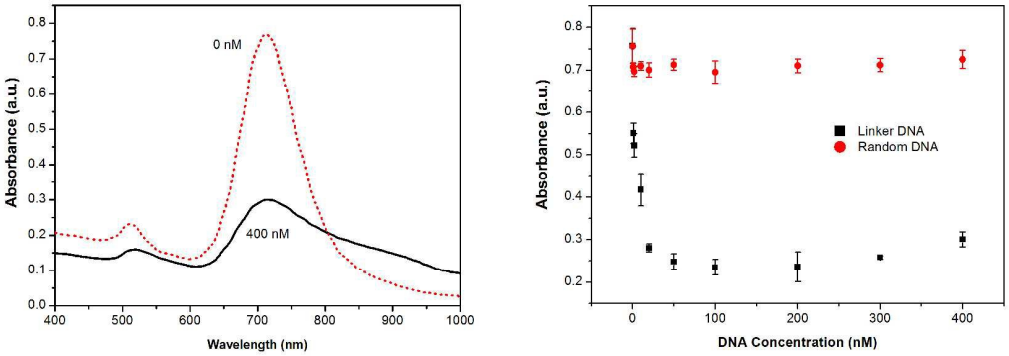

Fig. 3 UV-vis absorption spectra of GNR-DNA probes after reacting with 0 nM and 400 nM of linker DNA; UV-vis absorption intensity of GNRs at 708 nm after reaction with different amount of linker DNA and random DNA

probes had little change after DNA functionalization, demonstrating dispersed GNR probes obtained without aggregation.[44] Meanwhile, average hydrodynamic size of GNRs that determined by DLS technique increased from 65.8 nm to 78.8 nm and 76.5 nm after DNA modification, illustrating successful construction of GNR-3'-DNA and GNR-5'-DNA probes. Furthermore the average number of DNA loading per nanorod was calculated as 251 with a 6-carboxyfluorescein and thiol dual labeled DNA, following the same fabrication procedure (details please see ESI). Thus high overall yield of GNR-DNA probes was demonstrated.

Optimization of GNR assembly

The decorated 3'-thiolated DNA and 5'-thiolated DNA on side sites of GNR probes were suppose to hybridize with linker DNA under right conditions according to our design, resulting in side-by-side assembly of nanorods. Therein adding amount of linker DNA is critical for hybridization and assembly. Different final concentrations of linker DNA from 0 to 400 nM were initially used to obtain assemblies and analyzed for optimal condition. As shown in absorption spectra of Fig. 3, a red-shift of transverse peak and blue-shift of longitudinal peak of GNRs was observed while large amount of linker DNA (400 nM) was added, companying with a significant decrease in absorption intensity of longitudinal peak. On the contrary, there was no significant change in the absorption intensity of UV-vis spectra while different amount of random DNA was added. It was demonstrated that GNR assemblies were fabricated in Tris buffer induced by hybridization of linker DNA and thiolated DNA on the GNR probes, since the absorption spectra was in accordance with previous reports.[21, 27]
Moreover the absorption intensity of GNRs at 708 nm (longitudinal peak wavelength of GNR-DNA probes) decreased initially (0-100 nM) and then increased slowly (>100 nM) with the increasing concentration of linker DNA, as displayed in Fig. 3. It indicated that the configuration and yield of GNR side-by-side assemblies significantly depended on the concentration of linker DNA. As reported by EI-Sayed's team, there is a linear relationship between absorption maximum of longitudinal SPR peak and mean aspect ratio of GNRs experimentally and theoretically.[43] Moreover the particle concentration in buffer also has a lot of influence on the absorption intensity.[44] Both would attribute to the observed change of absorption spectra. Most probably, with the increasing concentration of linker DNA (0-100 nM), the number and size of GNR assemblies increased and reached saturation gradually. While abundant linker DNA was added (>100 nM) and mixed with GNR probes simultaneously, excess linker DNA hybridized with 3' and 5'-thiolated DNA on side sites of GNR probes sufficiently. And it would be more difficult for linker DNA to hybridize with two types of GNR probes at the same time, resulting in slight increase in the number of dispersed GNRs. The mean aspect ratio of GNRs and particle concentration in buffer decreased initially as a result of increasing side-by-side GNR assembly, and then increased resulted by increasing dispersed GNRs. Thus linker DNA with an optimal concentration of 100 nM was applied for further quantitative analysis.
GNR side-by-side assemblies could also be directly characterized using TEM images. Fig. 4 shows the structure variation of the side-by-side assembly of nanorods reacting with 5 and 100 nM of linker DNA. Large GNR ladders were observed while adding with 100 nM of linker DNA. Besides, hydrodynamic diameters by DLS measurements also significantly changed after adding and reacting with different amount of Linker DNA. As shown in ESI Fig. S1, the average diameter of GNR assemblies induced by 100 nM of linker DNA was 342 nm. However the average hydrodynamic diameter of assemblies induced by 5 nM of linker DNA was only 106 nm that was much smaller, in accordance with TEM and spectral analysis.

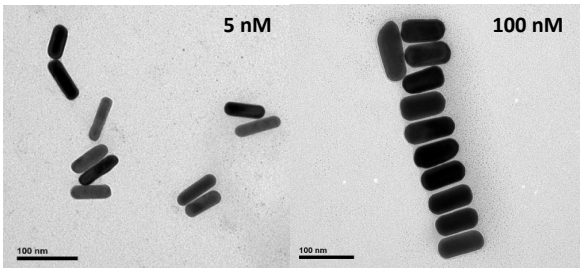

Fig. 4 Representative TEM pictures of GNR side-by-side assemblies added with 5 nM and 100 nM of linker DNA

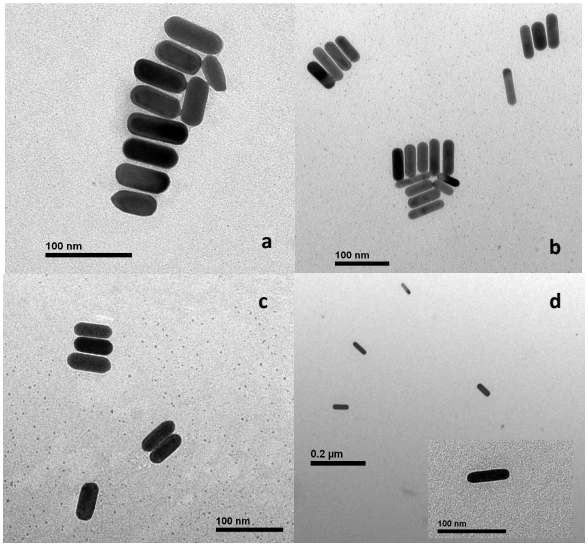

Fig.5 Representative TEM images of GNRs after reaction with different concentrations of OTA (a to d: 0, 2, 10 and 20 ng/mL) and 100 nM linker DNA

Analytical performance of proposed aptasensor

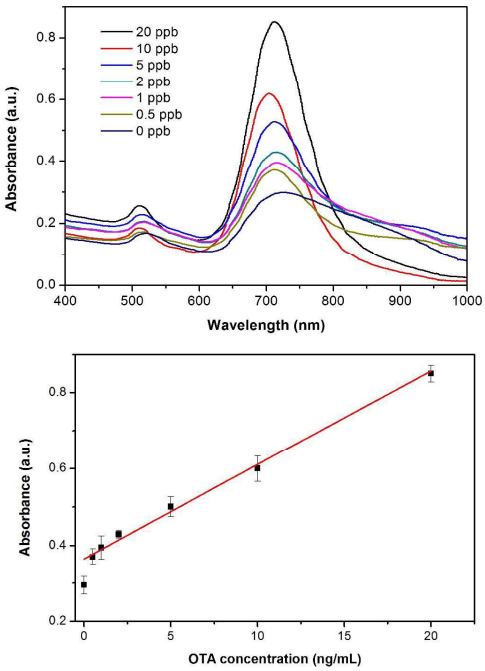

Fig.6 UV-vis absorption spectra and calibration curve of GNR assemblies with different concentrations of OTA standard solution (0, 0.5, 1, 2, 5, 10 and 20 ng/mL or ppb)

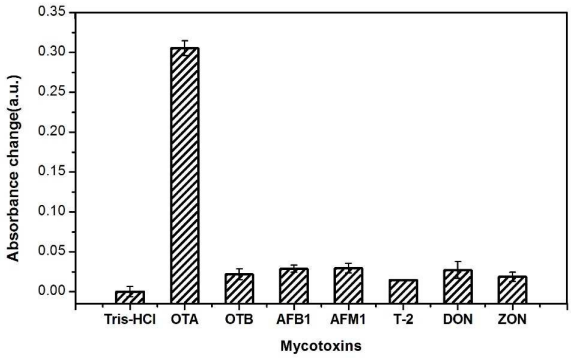

Fig. 7 Selectivity evaluation of fabricated aptasensor with other mycotoxins

Fig. 5 displays the representative TEM images of GNR probes after reaction with increasing concentration of OTA (0, 2, 10 and 20 ng/mL) and 100 nM of linker DNA. In the presence of OTA molecule (2 ng/mL), a small number of GNR ladders or dispersed GNRs were observed in solution. With increasing addition amount of OTA (10 and 20 ng/mL), more dispersed GNRs were obtained. And hydrodynamic diameters of GNR probes after reaction and number of nanorods in assemblies through statistical analysis were shown in ESI Fig. S2 and Fig. S3, respectively. It was demonstrated that, OTA molecules

Table 2 Determination of OTA in red wine samples

Sample	Spiked (ng/mL)	Detected Mean±SD (ng/mL)	Recovery (%)
Sample 1	2.0	2.364±0.304	118.2
Sample 2	5.0	5.205±0.532	104.1
Sample 3	10.0	9.204±0.876	92.0
Sample 4	20.0	18.644±1.130	93.2

SD represents standard deviation

specifically recognized by aptamer in the Tris-HCl buffer (pH 8.5). Thus linker DNA was not strong enough to hold GNR-5'-DNA probe, leading to decreased number of GNR ladders. More GNRs dispersed in solution with increased recognition of aptamer-OTA and decreased interparticle DNA hybridization.

Fig. 6 shows that the absorption spectra of GNRs varied with various OTA concentrations in the range of 0 to 20 ng/mL, induced by changes in configuration and amount of GNR assemblies. It is clearly shown that, with the decreasing of OTA concentration, longitudinal peak of GNRs blue shifted at first and then red shifted, accompanying with decreasing of absorption intensity. A significant band-broadening of longitudinal peak and another SPR peak over 900 nm were also be observed, while the OTA concentration was lower than 5 ng/mL. The result illustrated that larger side-by-side assemblies were fabricated with lower concentration of OTA. And the absorption intensity especially fixed wavelength at 708 nm, was used for further quantitative analysis.

The sensitivity of the developed optical aptasensor based on GNR side-by-side assembly was determined based on 3σ rule. The data were linearly correlated with equation $Abs=0.025C_{OTA}+0.37$ with a correlation coefficient of 0.98 in the concentration range of 0.5 to 20 ng/mL (as shown in Fig. 6). And the limit of detection (LOD) of this approach was calculated as 0.22 ng/mL (0.5 nM) in subnanomolar level, which could meet the need for detection of the allowed OTA in foods ready for retail sale according to the European Commission standards (2 ng/g) [45, 46] and China (5 ng/g). [47]

In order to evaluate the selectivity of established OTA aptasensor, other common toxic mycotoxins in agri-produces and food including OTB, AFB_1, AFM_1, T-2 toxin, DON and ZON, with concentration of 10 ng/mL were tested using proposed aptasensor. And the change of absorption intensity of GNRs at 708 nm between other mycotoxins and negative sample (Tris-HCl buffer) after reaction was much smaller than that of OTA (≤9.7% of OTA response) as shown in Fig. 7. Thus, it was demonstrated that optical aptasensor based on GNR side-by-side assembly had good performance on selectivity towards OTA detection.

Detection of OTA in red wine samples

The proposed aptasensor was applied for OTA determination in real red wine samples, for feasibility evaluation. The wine

samples purchased from local supermarket were spiked with different concentration of OTA (2, 5, 10 and 20 ng/mL) and then extracted using a two-step procedure for aptasensor analysis. A non-artificial contaminated red wine sample was used as blank sample. The detection results are summarized in Table 2. According to the results, recoveries of OTA in red wine samples were detected in the range of 92.0%-118.2%. The feasibility of developed aptasensor was evaluated, indicating it had a promising feature for practical use of OTA detection in real wine samples.

Conclusions

In summary, GNRs have been successfully oriented side-by-side assembled to develop a new optical aptasensor for OTA determination. Linker DNA containing aptamer sequences specifically recognized OTA molecules. Otherwise Linker DNA hybridized with compromised DNA on the side sites of nanorods, leading to oriented GNR assembly. OTA could be detected at low concentration linearly ranged from 0.5 to 20 ng/mL based on absorption intensity of UV-vis spectra, induced by conformational and number changes of GNR assemblies. The obtained subnanomolar LOD was lower than the maximum food safety limit and was achieved without requiring expensive and sophisticated equipment or highly qualified operator. The proposed aptasensor based on GNR assemblies was simple, efficient, selective and cost-effective with only one-step detection procedure, which would hold great potential for OTA determination in real red wine samples. Thereby it would be a promising alternative to toxin screening strategy to guarantee food safety in the future.

Acknowledgements

The authors are thankful to the 985-Institute of Agrobiology and Environmental Sciences at Zhejiang University, for providing convenience in use of their facilities and equipment. This work was financially supported by National Nature Science Foundation of China (No.31401572), China Postdoctoral Science Foundation (Grant No. 2014M551750 and 2015T80617) and Public Welfare Technology Applied Research Project of Zhejiang Province (No. 2014C32002).

References

1 A. Pfohl-Leszkowicz and R. A. Manderville, *Mol. Nutr. Food Res.*, 2007, **51**, 61-99.
2 E. Petzinger and K. Ziegler, *J. Vet. Pharmacol. Ther.*, 2000, **23**, 91-98.
3 C. M. Maragos, *Toxin Rev.*, 2004, **23**, 317-344.
4 A. Rhouati, C. Yang, A. Hayat and J.-L. Marty, *Toxins*, 2013, **5**, 1988-2008.
5 S. Song, L. Wang, J. Li, C. Fan and J. Zhao, *TrAC Trend. Anal. Chem.*, 2008, **27**, 108-117.
6 J. A. Cruz-Aguado and G. Penner, *J. Am. Chem. Soc.*, 2008, **56**, 10456-10461.
7 J. A. Cruz-Aguado and G. Penner, *Anal. Chem.*, 2008, **80**, 8853-8855.
8 C. Yang, V. Lates, B. Prieto-Simón, J.-L. Marty and X. Yang, *Talanta*, 2013, **116**, 520-526.
9 L. Jiang, J. Qian, X. Yang, Y. Yan, Q. Liu, K. Wang and K. Wang, *Anal. Chim. Acta*, 2014, **806**, 128-135.
10 T. H. Ha, *Toxins*, 2015, **7**, 5276-5300.
11 J. H. Soh, Y. Lin, S. Rana, J. Y. Ying and M. M. Stevens, *Anal. Chem.*, 2015, **87**, 7644-7652.
12 D. Afzali, F. Fathirad and S. Ghaseminezhad, *J. Food Sci. Technol.*, 2016, **53**, 909-914.
13 E.-J. Jo, H. Mun, S.-J. Kim, W.-B. Shim and M.-G. Kim, *Food chem.*, 2016, **194**, 1102-1107.
14 C. Yang, Y. Wang, J.-L. Marty and X. Yang, *Biosens. Bioelectron.*, 2011, **26**, 2724-2727.
15 L. Vigderman, B. P. Khanal and E. R. Zubarev, *Adv. Mater.*, 2012, **24**, 4811-4841.
16 M. Grzelczak, J. Perez-Juste, P. Mulvaney and L. M. Liz-Marzan, *Chem. Soc. Rev.*, 2008, **37**, 1783-1791.
17 H. Chen, L. Shao, Q. Li and J. Wang, *Chem. Soc. Rev.*, 2013, **42**, 2679-2724.
18 X. Xu, X. Liu, Y. Li and Y. Ying, *Biosens. Bioelectron.*, 2013, **47**, 361-367.
19 X. Xu, Y. Ying and Y. Li, *Sens. Actuators B: Chem.*, 2012, **175**, 194-200.
20 L. Wang, L. Xu, H. Kuang, C. Xu and N. A. Kotov, *Acc. Chem. Res.*, 2012, **45**, 1916-1926.
21 L. Wang, Y. Zhu, L. Xu, W. Chen, H. Kuang, L. Liu, A. Agarwal, C. Xu and N. A. Kotov, *Angew. Chem. Int. Ed.*, 2010, **49**, 5472-5475.
22 K. Caswell, J. N. Wilson, U. H. Bunz and C. J. Murphy, *J. Am. Chem. Soc.*, 2003, **125**, 13914-13915.
23 K. G. Thomas, S. Barazzouk, B. I. Ipe, S. S. Joseph and P. V. Kamat, *J. Phys. Chem. B*, 2004, **108**, 13066-13068.
24 W. Ma, H. Kuang, L. Xu, L. Ding, C. Xu, L. Wang and N. A. Kotov, *Natu. Commun.*, 2013, **4**.
25 S. Pal, Z. Deng, H. Wang, S. Zou, Y. Liu and H. Yan, *J. Am. Chem. Soc.*, 2011, **133**, 17606-17609.
26. Z. Li, Z. Zhu, W. Liu, Y. Zhou, B. Han, Y. Gao and Z. Tang, *J. Am. Chem. Soc.*, 2012, **134**, 3322-3325.
27 H.-H. Cai, D. Lin, J. Wang, P.-H. Yang and J. Cai, *Sens. Actuators B: Chem.*, 2014, **196**, 252-259.
28 Y. Wang, Y. F. Li, J. Wang, Y. Sang and C. Z. Huang, *Chem. Commun.*, 2010, **46**, 1332-1334.
29 Y. Zhu, L. Xu, W. Ma, Z. Xu, H. Kuang, L. Wang and C. Xu, *Chem. Commun.*, 2012, **48**, 11889-11891.
30 J.-Y. Chang, H. Wu, H. Chen, Y.-C. Ling and W. Tan, *Chem. Commun.*, 2005, 1092-1094.
31 S. J. Zhen, C. Z. Huang, J. Wang and Y. F. Li, *J. Phy. Chem. C*, 2009, **113**, 21543-21547.
32 J. Wang, P. Zhang, J. Y. Li, L. Q. Chen, C. Z. Huang and Y. F. Li, *Analyst*, 2010, **135**, 2826-2831.
33 M. Liu and P. Guyot-Sionnest, *J. Phys. Chem. B*, 2005, **109**, 22192-22200.
34 B. Nikoobakht and M. A. El-Sayed, *Chem. Mater.*, 2003, **15**, 1957-1962.

35 T. K. Sau and C. J. Murphy, *J. Am. Chem. Soc.*, 2004, **126**, 8648-8649.
36 C. J. Murphy, T. K. San, A. M. Gole, C. J. Orendorff, J. X. Gao, L. Gou, S. E. Hunyadi and T. Li, *J. Phys. Chem. B*, 2005, **109**, 13857-13870.
37 X. Geng, D. Zhang, H. Wang and Q. Zhao, *Anal. Bioanal. Chem.*, 2013, **405**, 2443-2449.
38 Z. Zhu, M. Feng, L. Zuo, Z. Zhu, F. Wang, L. Chen, J. Li, G. Shan and S.-Z. Luo, *Biosens. Bioelectron.*, 2015, **65**, 320-326.
39 C. Yang, V. Lates, B. Prieto-Simón, J.-L. Marty and X. Yang, *Biosens. Bioelectron.*, 2012, **32**, 208-212.
40 J. Liu and Y. Lu, *Nat. Protoc.*, 2006, **1**, 246-252.
41 L. Tang, S. Li, F. Han, L. Liu, L. Xu, W. Ma, H. Kuang, A. Li, L. Wang and C. Xu, *Biosens. Bioelectron.*, 2015, **71**, 7-12.
42 L. Xu, H. Kuang, C. Xu, W. Ma, L. Wang and N. A. Kotov, *J. Am. Chem. Soc.*, 2012, **134**, 1699-1709.
43 S. Link, M. Mohamed and M. El-Sayed, *J. Phys. Chem. B*, 1999, **103**, 3073-3077.
44 C. Yu and J. Irudayaraj, *Anal. Chem.*, 2007, **79**, 572-579.
45 *Off. J. Eur. Union*, 2006, **L 364**, 5-24.
46 *Off. J. Eur. Union*, 2012, **L 176**, 43-45.
47 J. N. Selvaraj, Y. Wang, L. Zhou, Y. Zhao, F. Xing, X. Dai and Y. Liu, *Food Addit. Contam. A*, 2015, **32**, 440-452.

Graphical Abstract

In this work, a new aptasensor based on gold nanorod (GNR) side-by-side assembly was studied for one-step determination of ochratoxin A (OTA).